



Investigating the efficiency of surfactant-modified zeolites@pumice to remove phosphate from synthetic wastewater using Box-Behnken design

Sadegh Ghasemi^a, Ehsan Derikvand^{a,*}, Saeb Khoshnavaz^a, Saeed Boroomand Nasab^b, Mohsen Solimani Babarsad^a

^aDepartment of Civil Engineering- Water Resources Engineering and Management, Shoushtar Branch, Islamic Azad University, Shoushtar, Iran, Tel. +98 613 6232491, email: sadeghghasemi23@gmail.com (S. Ghasemi), ederikvand@yahoo.com (E. Derikvand), saeb.khoshnavaz@gmail.com (S. Khoshnavaz), Mohsen.solb@gmail.com (M.S. Babarsad)

^bDepartment of Irrigation and Drainage Engineering, Shahid Chamran University, Ahvaz, Iran, Tel. +98 611 3330635, email: boroomandsaeed@yahoo.com (S.B. Nasab)

Received 23 April 2018; Accepted 20 October 2018

ABSTRACT

The discharge of phosphorus into surface waters results in overgrowth of aquatic plants and consequent eutrophication of rivers and seawaters; thus, removing this material to prevent surface-water nutrient uptake has received researchers' attention in recent years. The aim of the present study was to investigate the efficiency of stabilization of zeolite nanoparticles modified by cationic surfactant on pumice aggregates to remove phosphate from aquatic environments. In this study, zeolite nanoparticles, modified by CTAB surfactant, were stabilized on pumice aggregates substrate using heating operation; then, the structural and physical features of the prepared absorbent were analyzed using FTIR, XRD, SEM, and EDAX techniques. Experiments were designed using Box-Behnken response surface methodology to improve the variables. Variables of pH (5–9), temperature (15–45°C), and amount of absorbent (5–15 g/L) were investigated. In addition, in order to investigate kinetics and adsorption isotherm, separate tests were conducted to determine the optimal amount of contact time (5–150 min) and phosphate concentration (5–28 mg/L). Results show that the optimum conditions to remove phosphate by modified aggregates were measured at a pH of 5; temperature of 45°C and absorbent amount of 15 g/L. Kinetics investigations showed that phosphate removal follows the second-order model and the optimum contact time was measured at 60 min in which phosphate removal efficiency was 82.22%. The results also show that phosphate adsorption isotherm has good agreement with Langmuir isotherm. The study shows that stabilizing the modified zeolite nanoparticles using cationic surfactant on pumice aggregate is highly effective for phosphate removal, thus it can be used for removing such pollutants from aquatic environment.

Keywords: Phosphate; Pumice; Modified zeolite; Kinetics and adsorption isotherm

1. Introduction

Phosphorus is usually discharged into the environment as phosphate. Large amount of phosphate is used in various industries such as pesticides, fertilizer, metallurgy, food, detergents, drugs, soft and cold drinks etc. [1]. Undoubtedly, disproportionate use of phosphates

including mineral phosphates (ortho and polyphosphate) and organic phosphate (like detergents) produces large amount of phosphate containing wastes, which are dumped directly into aquatic environments [2]. Although phosphate is among the necessary elements for the growth of animals and plants on the planet earth, discharging more than 0.02 mg/L of phosphorus into aquatic systems, especially lakes and still waters leads to eutrophication, growth of algae and aquatic plants, and the death of aquatic organisms in the end [3,4]. In addition to phos-

*Corresponding author.

phate, nitrate, sunlight and carbon dioxide are involved in elevated nutrient uptake phenomenon; however, phosphate is the key factor due to restrictive feature [5]. In general, reducing extra phosphate from wastewater before discharging into surface waters is considered as the first measure. Thus, most of the recent studies have focused on phosphate removal from water [6,7]. Phosphorus compounds can be removed using various methods including ionic exchange, adsorption, micro filtration, coagulation and deposition [8]. Recently, absorption processes have been favored considerably due to high efficiency, non-toxicity, being simple, availability of wide range of absorbents, and the possibility of extensive use within concentrations range [9]. Various absorbents have been used for phosphate ions removal including fly ash [10], slag [11], alginate [12], bentonite [13], cellulose [14], lanthanum oxide [15], active charcoal [16], modified egg shell [17], chitosan [18], calcified pyrite [19], graphene oxide [20], carbon mesoporous [21], etc. However, most studies have focused on selecting inexpensive absorbents, such as local minerals, to remove water pollutants. These absorbents can be used either in natural or modified forms; pumice and zeolite are among these cheap absorbents [22,23]. Pumice is a light and porous volcanic rock; it has a high surface area and is found easily and cheaply in nature. Pumice is among those volcanic rock that have been considered for environmental pollutant removal due to porous and non-crystalline structure and containing large amount of silica oxide and aluminum [24]. In addition, zeolites are a group of micro porous aluminosilicate that are made naturally in the environment. Having a high specific surface area, zeolites can be used potentially for cases such as adsorption of pollutants [25]. Regarding the aluminosilicate structure, zeolite and pumice are negatively charged [26,27]; while modified by cationic surfactant, their surface charge is changeable [28]. Due to the characteristics of cationic surfactants, these compounds tend to undergo negative interactions, which make them a good option for external surface modification of various materials and boosting their anion exchange capacity [29]. For example, Akbal investigated the absorption of phenol and 4-chlorophenol using modified pumice rock by surfactant and unmodified natural aggregate from aquatic solutions; the results show that unmodified natural pumice cannot absorb phenol compound. Nevertheless, modified pumice was highly efficient in absorption of phenol and 4-chlorophenol [30]. According to the points mentioned above, the most important limiting factor in the use of pumice aggregates is their low potential in absorbing mineral anionic pollutants such as phosphate in water. Research studies showed that if the nanoparticles are stabilized on the surface of porous materials, a new material will be formed which undoubtedly possess some of the unique features of nanoparticles and porous material and it will increase the performance in absorbing the pollutants. Thus, the aim of the present study is to achieve an efficient method for enhancing the efficiency of pumice aggregates.

In this regard, the authors tried to investigate the removal of phosphate using Box-Behnken response surface methodology from synthetic aquatic solutions by stabilizing the modified zeolite using cationic surfactant CTAB ($C_{19}H_{42}NBR$) on pumice aggregates.

2. Materials and methods

2.1. Granulation and activation of pumice aggregates

Pumice aggregates were prepared from local mines; then, they were crushed and granulated in sizes of 4 to 6 mm by graded sieve. In order to remove impurities in minerals for boosting the active contact surface and enhanced efficiency, aggregates were floated in hydrochloric acid (1 N) afterwards. After 24 h, aggregates were removed from the acid and were washed 7 times on average with non-ionized water in order to remove the remaining acid and allowing the pH of the water to reach 7. Next, these aggregates were put into the furnace for 3 h under 750°C for calcination and creating an inner expansion within the aggregates and opening of the porous channels.

2.2. Preparation and modification of zeolite nanoparticles

Zeolite mineral samples, used by mine reserves of Semnan city in the central part of Semnan province, Iran, were provided in powder. In this study, natural nanoparticles of zeolite mineral were prepared by Planetary Ball Mill; this is a suitable method for particle size reduction [31]. To this end, powered samples of zeolite were grounded by Planetary Ball Mill (Model: PM 400-RETSCH) for 100 h at 300 rpm. After preparing the nanoparticles, zeolites were converted into cationic zeolite using CTAB surfactant [$(C_{16}H_{33})N(CH_3) Br$] according to the study of Wang et al. [32] with some minor modifications. Given the amount of CMC (Critical Micelle Concentration) of CTAB surfactant, which is 0.92 mM [33], 10 g of nanoparticles was added to 100 ml of CTAB solution with the concentration of 9.2 mmol·l⁻¹ to modify the zeolite nanoparticles (the concentration of the solution was set at 0.92 mM per gram of the absorbent). This mixture was kept at room temperature for 24 h at 140 rpm. Next, nanoparticles were separated by the centrifuge machine and were dried in an oven for 8 h at 90°C. Finally, the particle size analyzer machine (Model: Scatterscop Codex 1) and Fourier infrared spectroscopy (Model: Perkin Elmer BX-II) were used to investigate the particle size and spectroscopy of modified nanoparticles, respectively.

2.3. Stabilization of modified zeolite nanoparticles on pumice aggregates

In order to stabilize the modified zeolite nanoparticles on pumice aggregates, the loading ratio of 10 wt% nanoparticles to aggregates was used. To this aim, 10 g of modified zeolite nanoparticles was dissolved in 200 ml of distilled water. A 10% suspension of modified zeolite nanoparticles was mixed on a magnetic mixer for 30 min. Then, it was exposed to ultrasonic waves using ultrasonic bath (Model: Starsonic18–35) at the frequency of 50 kHz for 30 min to make the zeolite nanoparticles separate thoroughly. Next, 100 g of pumice aggregates was added to this suspension and it was then put on a shaker machine for 18 h at 120 rpm to make the mixture scatter homogeneously and evenly. Next, the prepared mixtures were exposed to temperatures of 450°C (90 min) and 650°C (90 min) to allow the nanoparticles suitably stabilize on the aggregates. Eventually, in order to investigate stabilization status and coverage of

zeolite nanoparticles on pumice aggregates, XRD (Model: Philips, PW 1840), EDAX (Model: ZEISS, SIGMA VP-500) and SEM (Model: Philips, XL30) methods were applied.

2.4. Designing the tests using Box-Behnken to optimize factors affecting phosphate removal

In this study, in order to investigate the factors affecting phosphate removal process by stabilization of cationic modified zeolite nanoparticles on pumice aggregates and to optimize three parameters of pH, temperature, and adsorbent amount, tests were designed using Box-Behnken response surface method. For this purpose, a 3 variable design with 3 levels and 3 central points was applied using Minitab17 software. Overall, 15 tests were designed and conducted. Table 1 shows the level of independent variables and their values.

2.5. Tests procedures

Mono potassium phosphate salt (KH_2PO_4), produced by the Samchun Pure Chemical Co., was used for preparing the solutions. First, phosphate 1 L solutions with the concentration of 18 mg/L were prepared with deionized water; the pH of the solutions was set by pH meter at the desired number (5, 7, or 9) using hydrochloric acid or sodium hydroxide. Then, the desired amount of the adsorbent (5, 10, and 15 g) was weighed by digital scale and added to the solutions; the heater within the designated case was turned on. After adjusting the temperature (15, 30, and 45°C), the solutions were mixed with a mixer for 30 min. Next, aggregates were separated from the solutions by filter paper. Finally, the filtered solution was gathered and the remaining phosphate was measured by Spectrophotometry method at 880 nm. It should be noted that all the tests were repeated at least three times and the average of data and results were used.

2.6. Investigation of adsorption isotherms

Adsorption isotherms have absorption features and equilibrium data; they explain how pollutants react with adsorbents. They play a role in boosting the adsorbent consumption; Langmuir and Freundlich isotherms are among the well-known isotherms [34]. Freundlich isotherm is achieved by assuming a heterogeneous surface and by non-monotonous distribution on the adsorbent surface, whereas the Langmuir isotherm indicates the single-layer

Table 1
Levels and values of independent variables

| Independent variables | Symbol | Low level (-1) | Mid-level (0) | High level (1) |
|------------------------|--------|----------------|---------------|----------------|
| pH | X_1 | 5 | 7 | 9 |
| Temperature (°C) | X_2 | 15 | 30 | 45 |
| Absorbent amount (g/L) | X_3 | 5 | 10 | 15 |

and monotonous absorption on the adsorbent surface. The linear form of the Langmuir equation is presented below [Eq. (1)] [35,36]:

$$\frac{1}{q_e} = \frac{1}{q_m} + \frac{1}{q_m \times K_1 \times C_e} \quad (1)$$

where q_e is the adsorbed dose at equilibrium (mg/g); q_m and K_1 are Langmuir parameters, which represent adsorption capacity (mg/g) and adsorption correlation energy, respectively. The basic features of Langmuir equation can be expressed by equilibrium parameter R_L [Eq. (2)] which is a dimensionless constant [37].

$$R_L = \frac{1}{1 + K_1 \times C_o} \quad (2)$$

R_L represents isotherm type; $0 < R_L < 1$ is desired adsorption; $R_L > 1$ undesirable adsorption; $R_L = 1$ linear adsorption and $R_L = 0$ irreversible adsorption [38]. The linear form of the Freundlich equation is given below [Eq. (3)] [39,40]:

$$\text{Log } q_e = \text{Log } K_f + \frac{1}{n} \text{Log } C_e \quad (3)$$

where K_f and n are the constants of Freundlich equation; they represent adsorption capacity (mg/g) and intensity of the adsorption, respectively. $n < 1$ indicates poor adsorption; $1 < n < 2$ average adsorption; $2 < n < 10$ desirable adsorption [41].

2.7. Investigation of adsorption kinetics

Kinetic models describe the process of adsorption reaction order based on the adsorption capacity [42]. First order adsorption kinetic model is explained by Eq. (4) [43]:

$$\text{Log}(q_e - q_t) = \text{Log } q_e + \frac{K_1}{2.303} t \quad (4)$$

Moreover, second order adsorption kinetic model is expressed by Eq. (5) [44]:

$$\frac{t}{q_t} = \left[\frac{1}{q_e} \right] t + \left[\frac{1}{K_2 \times q_e^2} \right] \quad (5)$$

where q_e (mg/g) and q_t (mg/g) are the adsorption capacity of the adsorbent at equilibrium condition and at time t , respectively. K_1 is equilibrium speed of first order adsorption (1/min) and k_2 equilibrium speed of second order adsorption (g/mg·min). Moreover, in the above equations, the adsorbed dose per gram of the adsorbent (adsorption capacity) is expressed by Eq. (6):

$$q_e = (C_o - C_e) \times \frac{V}{W} \quad (6)$$

where C_o (mg/L) is the adsorbed initial concentration, C_e (mg/L) concentration of the adsorbed after adsorption, V (L) solution volume and W (g) weight of the adsorbed.

2.8. Investigation of adsorption thermodynamic

Determining the parameters of thermodynamic of adsorption is another important criterion in describing process of adsorption. Enthalpy values (ΔH°) per kJ/mol, and entropy (ΔS°) per kJ/mol. K from gradient and y-intercept, diagram of $\ln K_L$ changes vs. $1/T$, are calculated based on Eq. (7) [45]:

$$\ln K_L = \frac{\Delta S^\circ}{R} - \frac{\Delta H^\circ}{RT} \quad (7)$$

where K_L is Thermodynamic equilibrium constant, R is universal gas constant (8.314 J/mol·K), and T is the absolute temperature per Kelvin. Meanwhile, the value of Gibbs free energy (ΔG°) per kJ/mol is achieved from Eq. (8) [46]:

$$\Delta G^\circ = -RT \ln K_L \quad (8)$$

3. Results and discussion

3.1. Investigating particle size and spectroscopy of the modified zeolite nanoparticles

According to the results of particle-size analysis, the sizes of d50 and d90 in zeolite sample were 37.6 and 60.1 nm, respectively. Fig. 1 shows the results of FTIR analysis on natural zeolite sample and modified zeolite by surfactant. In the

spectrum of natural zeolites, the bands observed in 446 and 607 cm^{-1} regions are related to the T-O bending vibrations (where T=Si or Al). In 794 and 1042 cm^{-1} the peaks observed are related to the T-O symmetric and asymmetric internal vibrations, respectively. Two peaks of 1636 and 3625 cm^{-1} relate to the presence of water molecules in zeolite structure; the former relates to the bending vibrations of water molecule and the latter relates to the symmetric stretching vibration of water molecule. Thus, it is confirmed that zeolite used in this experiment is a Clinoptilolite natural zeolite $[(K,Na,Ca)_6(AlSi)_{36}O_{72}] \cdot 20H_2O$. As shown in this figure, there are two extra peaks in the modified sample than the natural sample. These peaks are observed at 2361 and 3016 cm^{-1} regions, which are correspondent to the vibrations of C-C and C-H of CTAB surfactant molecular structure; these peaks are not observed in the natural zeolite. These bands indicate that CTAB organic cations have been absorbed in surfaces and between zeolite nanoparticle layers.

3.2. Investigating the purity and composition of stabilized zeolite nanoparticles modified on pumice aggregates

Fig. 2A presents XRD pattern of natural pumice aggregate sample. The mineralogy of its composition confirms the presence of diopside (in monoclinic crystal system with 23% of overall amount); olivine (in orthorhombic crystal system with 11% of overall amount), forsterite (mixture of manganese silicate with 15% of overall amount), cristob-

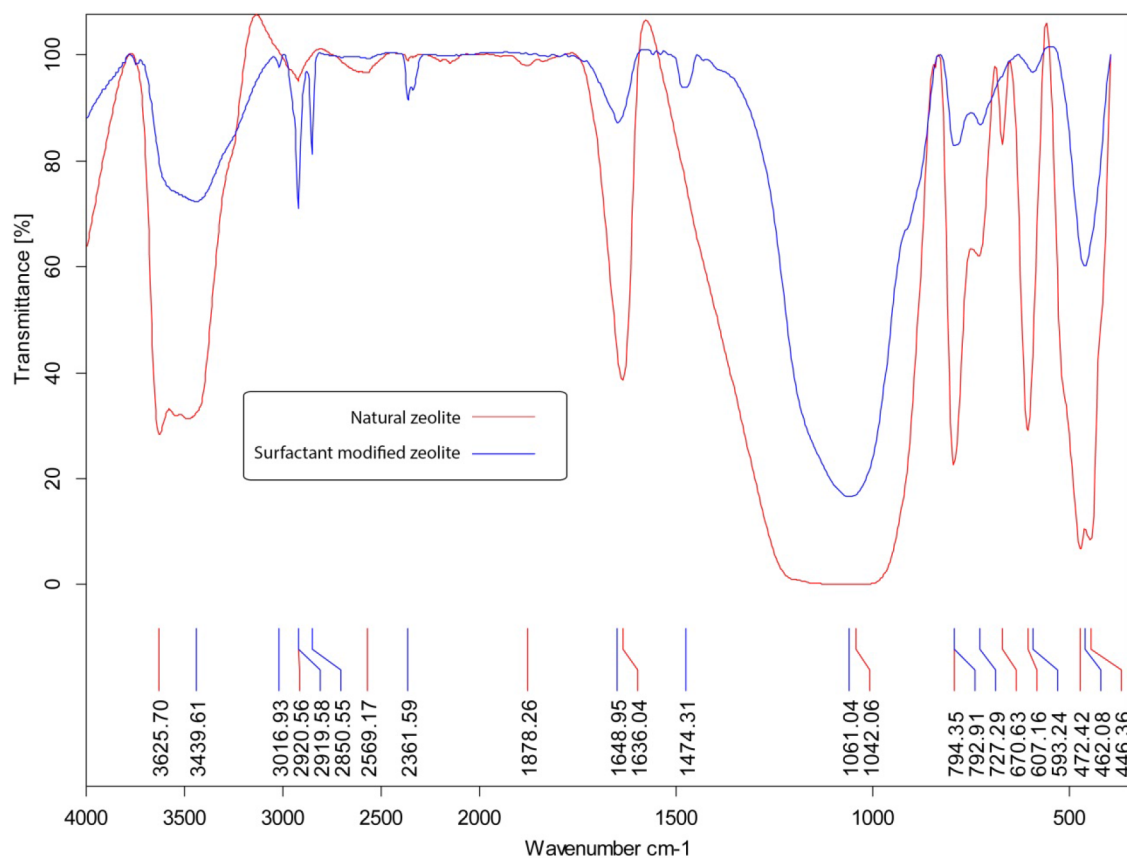


Fig. 1. FTIR analysis on natural and modified zeolite sample.

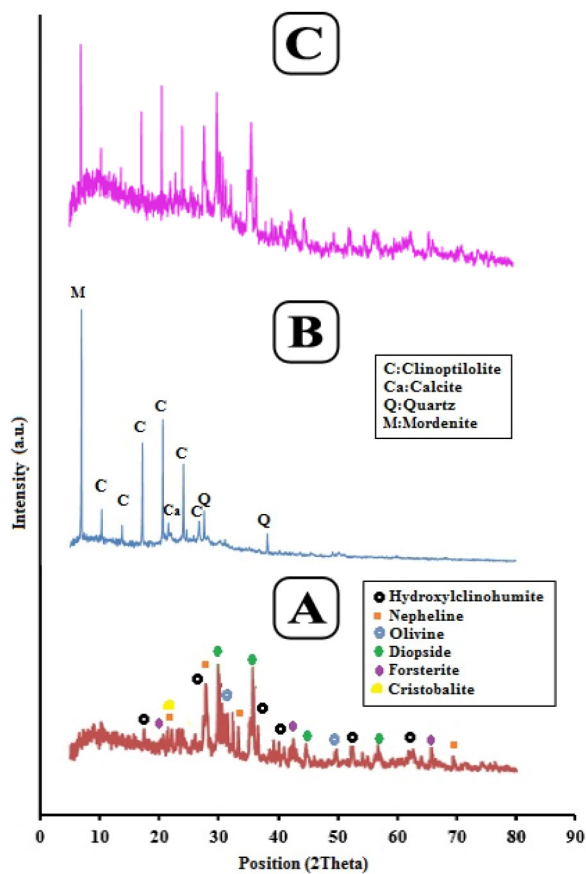


Fig. 2. X-ray diffraction pattern (A: pumice aggregates, B: modified zeolite nanoparticles, C: stabilized composite of zeolite nanoparticles modified on pumice aggregates).

alite (high temperature silica polymorph with 1% of overall amount), nepheline (in a hexagonal system with 21% of overall amount), and hydroxylclinohumite (in a monoclinic crystal system of humites group with 29% of the overall amount) in this mixture. Fig. 2B shows XRD diffraction pattern of the modified zeolite nanoparticles sample. Results show that clinoptilolite is the main crystalline phase of zeolite under study. The diffractions of this phase involve angles of 10.28, 13.71, 17.11, 20.05, 24.00, and 26.65. Furthermore, there are impurities of quartz (diffraction angles of 27.55 and 38.14), calcite (diffraction angle of 21.6), and mordenite (diffraction angle of 6.84) in the mixture. The sharp peaks with high intensity indicate that the crystalline structure of the mixture is complete. Fig. 2C shows the XRD pattern of the stabilized composite sample of the zeolite nanoparticles modified on pumice aggregates. The presence of both phases of the composite samples in the pattern is an indication of the successful formation of the synthesized composite. As shown in the figure, the intensity of zeolite peaks in the composite sample decreased than the pure dose. This difference shows the matrices interactions among the composite components. In the composite sample pattern, diffractions of pumice are mainly shown and only slight difference is observed in terms of the intensity of the diffractions; in other words, as zeolite amount increases, the underlying structure does not change and stays the same.

3.3. Investigating the morphology and elemental analysis of stabilization of zeolite nanoparticles modified on pumice aggregates

Table 2 presents the results of EDAX elemental analysis of natural pumice aggregates, zeolite nanoparticles and stabilized composite of zeolite nanoparticles modified on pumice aggregates. As shown, much of the weight percentage of the zeolite nanoparticle elements are made up of aluminum and silica (aluminosilicate) and significant increase in the dosage of these two elements on the composite sample surface is an indication of successful coverage of zeolite nanoparticles on pumice aggregates substrate.

Fig. 3 shows SEM (scanning electron microscope) pictures of natural pumice aggregates and stabilized composite of zeolite nanoparticles modified by pumice aggregate. It can be observed that zeolite nanoparticles lay on porous substrate of pumice aggregates as clods and masses. It is possible to observe the rugged surface and pores of pumice substrate easily; this rugged surface increases the adsorption capacity and specific surface area.

3.4. Results of tests designed by Box-Behnken model

Table 3 shows 15 tests designed by Box-Behnken model as well as values of variable, calculated removal percent and the model predicted values for phosphate removal; and then, the removal values of the tests were studied by Minitab17 software. Finally, the coefficients of the second order polynomial equation of the designed model, coefficients of the predicted regression for phosphate removal percentage, analysis of variance of data, response surface plots and the interval plots of the interactions among variables and optimum conditions for the desired pollutant were specified.

Table 4 shows the coded regression coefficients and predicted significance level by the model for phosphate removal by stabilized composite of zeolite nanoparticles modified by pumice aggregates. The correlation coefficient R^2 for phosphate removal by the model was measured at 0.9899, which is an indication of remarkable consistency between the results; it also shows that the model cannot predict only 1.01% of the variations.

According to the results of predicted regression for phosphate removal, the effects of variables of pH (X_1), the absorbent dose (X_3), temperature (X_2), and the interactions $X_2 \times X_2$, $X_3 \times X_3$ and $X_3 \times X_1$ were within the confidence level of 0.95. The coded second order polynomial equation obtained by Minitab17 software for phosphate removal is shown by Eq. (9):

$$Y = 55.533 - 6.975 X_1 + 8.188 X_3 + 4.213 X_2 - 0.229 X_1^2 - 3.504 X_3^2 - 2.554 X_2^2 - 2.00 X_3 X_1 - 0.950 X_1 X_2 + 0.975 X_3 X_2 \quad (9)$$

Based on the obtained equation and reported values of regression coefficients, it could be concluded that variables of the absorbent dose, pH and temperature, respectively had the highest effects on the phosphate removal efficiency. Removing the expressions that are not on the significant level, the final equation is defined as follows [Eq. (10)]:

$$Y = 55.533 - 6.975 X_1 + 8.188 X_3 + 4.213 X_2 - 3.504 X_3^2 - 2.554 X_2^2 - 2.00 X_3 X_1 \quad (10)$$

Table 2
Elemental analysis of pumice aggregates, natural zeolite and stabilized composite of zeolite nanoparticles modified on pumice aggregates

| Components | O | N | Si | Au | Na | Al | C | Ca | Mg | Fe | K |
|---|------|-----|------|-----|-----|-----|-----|-----|-----|-----|-----|
| Raw pumice aggregate weight% | 61 | 7.9 | 7.4 | 6.3 | 4.5 | 4.4 | 3.1 | 2.1 | 1.9 | 1.4 | – |
| Natural zeolite weight% | 68.3 | 3.4 | 14.9 | 2.8 | 4.7 | 3.2 | 1.2 | – | 0.7 | – | 0.8 |
| Stabilized composite of zeolite nanoparticles modified on pumice aggregates weight% | 60.4 | 3.6 | 13 | 3.3 | 6.2 | 5 | 2.5 | 1.9 | 1.4 | 1.6 | 1.1 |

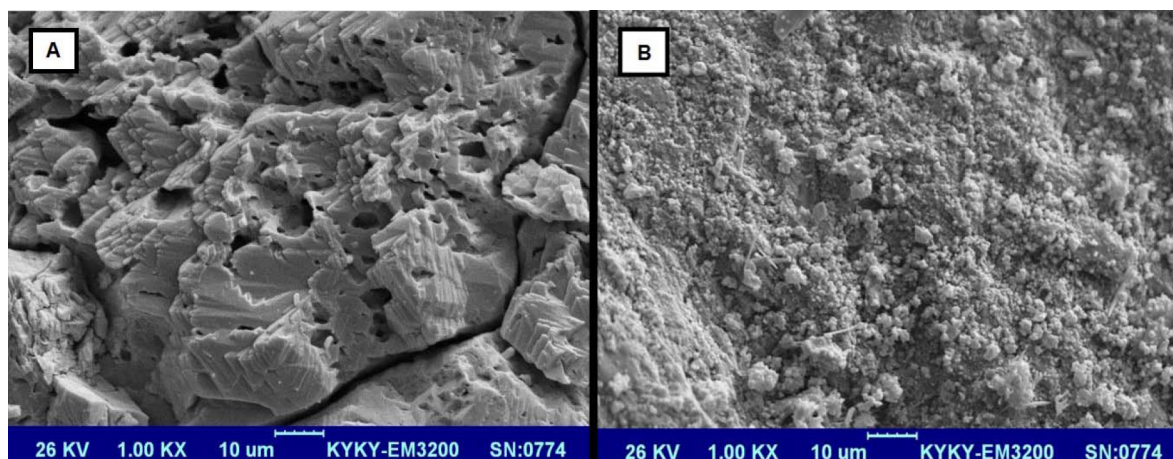


Fig. 3. SEM pictures (A: natural pumice aggregates, B: stabilized composite of zeolite nanoparticles modified on pumice aggregates).

Table 3
Box-Behnken design for phosphate removal by stabilized composite of zeolite nanoparticles modified on pumice aggregates

| Test number | pH (X_1) | Temperature ($^{\circ}\text{C}$) (X_2) | Absorbent dosage (g/L) (X_3) | Removal percentage | Predicted removal percentage |
|-------------|--------------|--|----------------------------------|--------------------|------------------------------|
| 1 | 9 | 30 | 5 | 38.1 | 38.6 |
| 2 | 5 | 30 | 15 | 69.5 | 68.9 |
| 3 | 9 | 45 | 10 | 50.2 | 49 |
| 4 | 7 | 30 | 10 | 55.4 | 55.5 |
| 5 | 5 | 45 | 10 | 65.9 | 64.8 |
| 6 | 7 | 45 | 15 | 61.3 | 62.8 |
| 7 | 5 | 15 | 10 | 53.4 | 54.5 |
| 8 | 9 | 15 | 10 | 41.5 | 42.5 |
| 9 | 7 | 15 | 15 | 53.1 | 52.4 |
| 10 | 7 | 30 | 10 | 55.1 | 55.5 |
| 11 | 7 | 30 | 10 | 56.1 | 55.5 |
| 12 | 7 | 45 | 5 | 43.9 | 44.5 |
| 13 | 9 | 30 | 15 | 51.4 | 51 |
| 14 | 5 | 30 | 5 | 48.2 | 48.5 |
| 15 | 7 | 15 | 5 | 39.6 | 38 |

3.4.1. The effect of pH on phosphate adsorption

The effect of pH parameter is investigated in this section of the study. Fig. 4 shows the diagram of response surface and interval between the interactive effects of pH and temperature with unchanged dosage of the absorbent (10 g/L)

on phosphate absorption rate. According to the results, as pH increased, the removal efficiency decreased at any given temperature. As shown in Fig. 5, an increase in pH at constant temperature of 30°C, decreased the removal efficiency at any given dosage of the absorbent. According to stud-

Table 4
Predicted regression coefficients and significance level of the parameters

| Term | Coefficient | P-value |
|------------------|-------------|---------|
| Constant | 55.53 | 0.000 |
| X_1 | -6.975 | 0.000 |
| X_2 | 4.213 | 0.001 |
| X_3 | 8.188 | 0.000 |
| $X_1 \times X_1$ | -0.229 | 0.785 |
| $X_2 \times X_2$ | -2.554 | 0.024 |
| $X_3 \times X_3$ | -3.504 | 0.007 |
| $X_2 \times X_1$ | -0.950 | 0.270 |
| $X_3 \times X_1$ | -2.00 | 0.048 |
| $X_3 \times X_2$ | 0.975 | 0.259 |

ies, in acidic pH, the concentration of H^+ in the solution is high; this cation causes positive charges on the surface of the adsorbent. Consequently, the adsorbent surface absorbs the phosphate (having negative charges) well in the acidic pH. At higher pH in alkaline medium, the concentration of OH^- is high and it creates negative charges on the surface of the adsorbent; thus, as phosphate pollutants are removed from the adsorbent surface, the removal efficiency

decreases. Previous studies have also shown that the zero point pH of pumice aggregates was reportedly within the range of 6.2 to 7.2 [47,48]. Since most of the phosphorus types are negative in aquatic medium, at pH lower than zero point, phosphorous adsorption rate increases due to positive charges of the adsorbent surface; at pH above zero point, phosphorous adsorption rate decreases due to negative charges of the adsorbent surface [49]. Thus, the optimum pH for phosphate predicted by the model is 5. Similar studies have been carried out in this regard; Kawasaki et al. investigated phosphate removal by aluminum hydroxide gel. They reported that phosphate removal was most efficient at pH of 5 [50]. Castaldi et al. studied the effects of pH on phosphate accumulation by red mud; they reported that phosphate removal was most efficient at pH of 4 [51].

3.4.2. The effect of the adsorbent dosage on phosphate adsorption

The effects of the adsorbent dosage on phosphate removal process were investigated within the range of 5 to 15 g/L. As shown in Fig. 5, increasing the adsorbent dosage at constant temperature of 30°C, increases the phosphate removal efficiency. Fig. 6 also shows that increasing the adsorbent dosage and temperature at constant pH of 7, increases the phosphate removal efficiency. These observations could be due to increased adsorbent spots and

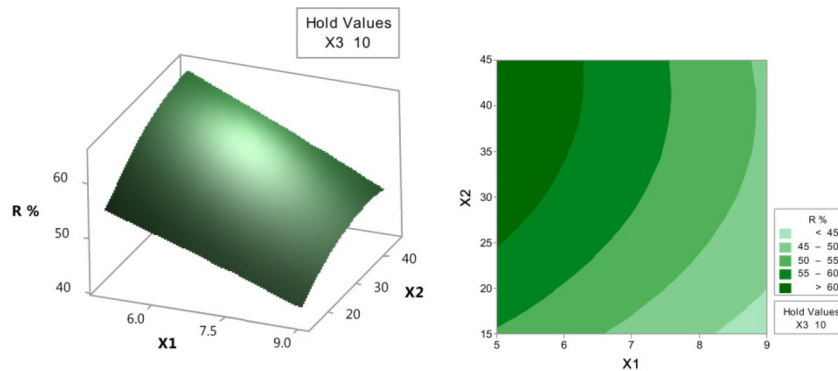


Fig. 4. The diagram of response surface and interaction interval of pH (X_1), temperature (X_2), and constant adsorbent dosage of 10 g/L (X_3) for phosphate removal.

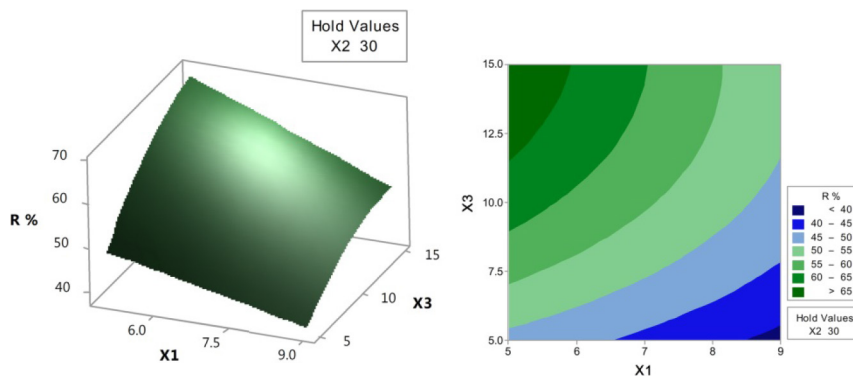


Fig. 5. The diagram of response surface and interaction interval of pH (X_1), adsorbent dosage (X_3), and constant temperature of 30°C (X_2) for phosphate removal.

absorbent surface groups and consequent increased of adsorption capacity. Naushad et al. and other researchers have reported similar results in this regard [52,53].

3.4.3. The effect of temperature on phosphate adsorption and determining thermodynamic features

The effects of temperature on phosphate removal were investigated within the range of 15–45°C. Fig. 4 shows that at constant dosage of the absorbent (10 g/L), as the temperature rises at all pH, phosphate removal increases. As shown in Fig. 6, at constant pH of 7, by increase in temperature at any given dosage of the absorbent, the removal efficiency increased; this could be due to increased mobility and ion collisions with the absorbent surface [54]. This increased removal efficiency, which is accompanied by temperature rise, is an indication of thermosensitive nature of the pollutant removal reaction. Thus, the optimum temperature predicted by the model for the maximum phosphate removal by the stabilized composite of zeolite nanoparticles modified by pumice aggregates is 45°C. In another study conducted by Rashid et al., phosphate removal by humic acid coated magnetite nanoparticles was investigated. They reported that temperature rise from 25 to 65°C increased the efficiency of phosphate removal [55]. In addition, Huang et al. investigated phosphate removal from wastewater using red mud; they tested the effects of temperature rise on phosphate removal within the ranges of 30–40°C, and concluded that temperature rise increased the adsorption capacity of the absorbent for phosphate removal [56].

In addition, the results of analyzing thermodynamics of absorption using the predicted model and considering the different values of temperature and keeping other parameters constant are given in Fig. 7 and Table 5.

According to the results, the positive value of ΔH° shows that the process of adsorption of phosphate by the stabilized composite of zeolite nanoparticles modified on pumice aggregates has been endothermic. The positive value of ΔS° shows that the irregularity value in the solution and random collisions have been increased during the adsorption of phosphate on the absorbent. Additionally, the values of ΔG° are all small and positive which show that they need little energy to conduct the adsorption of phosphate on the stabilized composite of zeolite nanoparticles

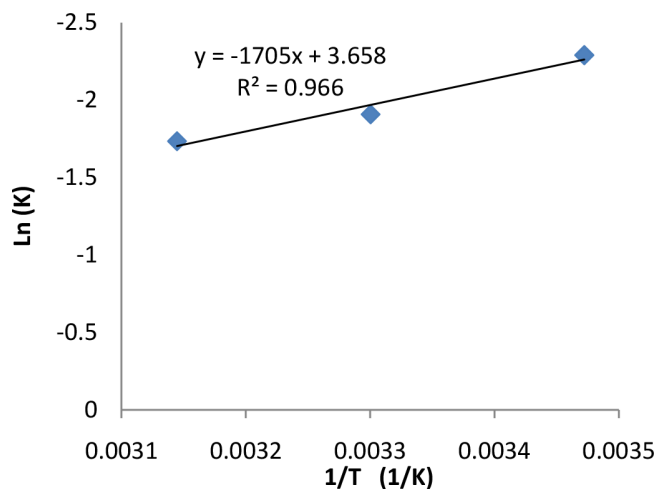


Fig. 7. The diagram of adsorption thermodynamic.

Table 5

The results of thermodynamic parameters of phosphate removal by the stabilized composite of zeolite nanoparticles modified on pumice aggregates (pH = 5, time = 30 min, absorbent dosage = 15 g/L and initial concentration = 18 mg/L)

| Temperature (K) | K_L (L/g) | ΔH° (kJ/mol) | ΔS° (kJ/mol.K) | ΔG° (kJ/mol) |
|-----------------|-------------|---------------------------|-----------------------------|---------------------------|
| 288 | 0.1012 | | | 5.483 |
| 303 | 0.1483 | 14.175 | 0.030 | 4.806 |
| 318 | 0.1764 | | | 4.586 |

modified on pumice aggregates [57]. It may not indicate the non-spontaneous process of phosphate removal on the absorbent, rather it shows that the absorbent at high temperature of 318 K can establish better performance in phosphate removal. Ozcan stated in his report on adsorption that acquiring positive values for ΔG° in the mechanism of ion-exchange is very conventional in the adsorption processes because the active compound of pollutant ions with absorbent may be shaped in the excited state [58]. Furthermore, acquiring the thermodynamic parameters through linear illustration of thermodynamic model can create a

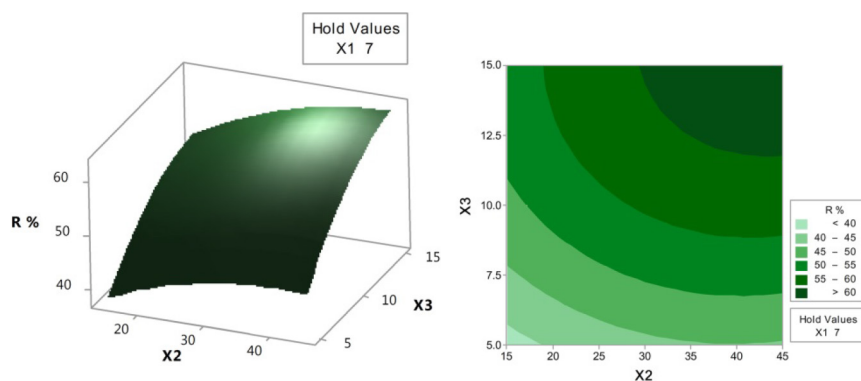


Fig. 6. The diagram of response surface and interaction interval of temperature (X_2), absorbent dosage (X_3), and constant pH of 7 (X_1) for phosphate removal.

variety of errors, which can cause replacements in the values achieved. When this happens in adsorption reactions, the small and negative values of ΔG° will transform into the small but positive values of ΔG° [59].

3.4.4. Process optimization

The parameters and optimal removal percentage of phosphate based on the results obtained from the Box-Behnken experimental design model are presented in Table 6. In order to validate the accuracy of the removal efficiency value obtained from the model, an experimental test was performed at the optimal points that the numerical value proximity of the results indicates the high accuracy of the model in predicting the results.

3.5. The effect of contact time on phosphate adsorption

In order to study and measure adsorption kinetics and determine the optimum value of contact time parameter, separate set of experiments were performed with different values of contact time (15, 30, 60, 90, 120, and 150 min) and keeping other parameters constant in the optimum conditions obtained by the model. Table 7 and Fig. 8 show the effects of contact time on the process of phosphate removal by the stabilized composite of zeolite nanoparticles modified by pumice aggregates under optimum conditions. According to the results, it can be concluded that increasing the contact time provided the phosphate ions with more opportunity to be absorbed by the adsorbent. It can also be inferred that maximum phosphate removal was

Table 6
Optimal parameters for removal of phosphate

| Optimal parameters | | | Phosphate removal percentage | |
|--------------------|------------------|------------------------|------------------------------|-------------------|
| pH | Temperature (°C) | Absorbent dosage (g/L) | Model prediction | Experimental test |
| 5 | 45 | 15 | 72.54 | 72.62 |

*The removal percentage results were obtained under condition of initial phosphate concentration = 18 mg/L and contact time = 30 min.

Table 7
Results of contact time on phosphate removal by the stabilized composite of zeolite nanoparticles modified on pumice aggregates

| Time (min) | Temperature (°C) | Absorbent dosage (g/L) | pH | Initial concentration (mg/L) | Secondary concentration (mg/L) | Removal percentage |
|------------|------------------|------------------------|----|------------------------------|--------------------------------|--------------------|
| 15 | 45 | 15 | 5 | 18 | 5.50 ± 0.072 a | 69.44 ± 0.40 a |
| 30 | | | | | 4.80 ± 0.065 b | 73.33 ± 0.36 b |
| 60 | | | | | 3.20 ± 0.081 c | 82.22 ± 0.45 c |
| 90 | | | | | 3.17 ± 0.075 c | 82.38 ± 0.41 c |
| 120 | | | | | 3.13 ± 0.065 c | 82.59 ± 0.36 c |
| 150 | | | | | 3.09 ± 0.080 c | 82.81 ± 0.44 c |

*Each mean value (± standard deviation) was obtained from three repetitions. Various letters in each specific column indicate significant difference in confidence level of 0.95 ($P < 0.05$).

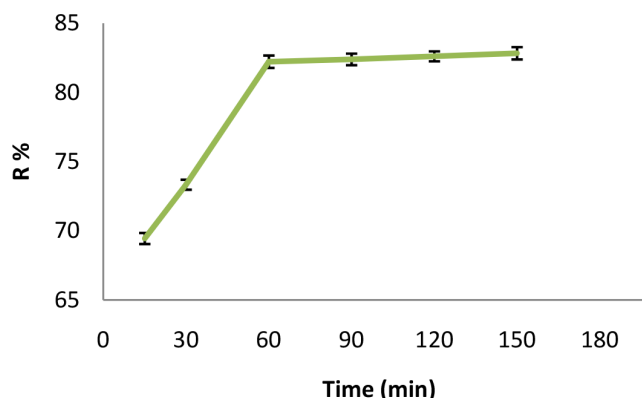


Fig. 8. The effects of contact time on phosphate removal by the stabilized composite of zeolite nanoparticles modified on pumice aggregates under optimum conditions (pH = 5, temperature = 45°C, and adsorbent dosage = 15 g/L) and the initial concentration of 18 mg/L.

performed within the first 60 min; removal was slowed down afterwards and reached equilibrium; in other words, the phosphate removal process consists of two steps. At the beginning of the experiments, it was fast but slowed down afterwards. Maybe, it is because there were numerous functional groups and adsorbent spots on the adsorbent surface at the beginning of the reaction and by passage of time, these spots were occupied and decreased in number. Results of analysis of variance and their comparison with Tukey method revealed that increasing the contact time increased removal efficiency; however, 60 min and more did not make a significant difference and it was considered as the optimum contact time for phosphate removal. Gan et al. investigated the effects of cetyltrimethyl ammonium bromide on the morphology of green synthesized Fe_3O_4 nanoparticles used to remove phosphate; they concluded that the modified adsorbent in a solution with concentration of 20 mg/L and adsorbent dosage of 2 g/L is capable of removing more than 80% of the phosphate in less than 30 min [60]. Karaca et al. conducted another study; they used raw and calcined dolomite for phosphate removal in aquatic solutions and reported that the equilibrium time of the adsorption process is approximately 30 min [61]. He et al. used lanthanum-incorporated porous zeolite for phos-

phate removal; they concluded that the equilibrium time in a solution with various concentrations of phosphate and adsorbent dose of 2 g/L was approximately 60 min [62].

3.5.1. Investigation of adsorption kinetics

Predicting the adsorption speed is the most important factor for adsorption process. Fig. 9 and Table 8 show the results of the first and second order phosphate adsorption kinetics. Based on the obtained parameter, it could be concluded that data follow the second order adsorption kinetic model because in the first order adsorption kinetics, R^2 values were desirable, but the value of tested q_e and calculated q_e were not equal, whereas in the second order adsorption kinetics, R^2 value was higher and more desirable and the value of tested q_e and calculated q_e were closer. Adherence of adsorption process of a second-order kinetics shows that the adsorption speed dependency on pollutant concentration is more and the speed of adsorption process is faster in contrast with the first-order kinetics and reaches its balance much sooner.

3.6. Investigating phosphate adsorption isotherm

Analysis and interpretation of adsorption isotherm is a key criterion for improving the adsorbent usage because equilibrium data are instrumental for design and function of absorption systems. Different set of experiments were performed using several values of initial phosphate concentrations (5, 10, 18, and 28 mg/L) and keeping other parameters constant under optimum conditions obtained by the

model to investigate and measure the prepared adsorbent isotherm and also tried to compare the improved performance of the modified pumice aggregates and performance of natural pumice aggregates in absorbing the phosphate pollutant. Table 9 and Fig. 10 show the effects of initial phosphate concentration on the adsorption capacity.

Comparison of natural pumice and modified pumice performances showed that adsorption capacity of natural pumice increased in different concentrations from 0.193 to 0.46 mg/g, whereas the adsorption capacity of the modified pumice increased from 0.321 to 1.04 mg/g, which shows the improved performance of modified adsorbent for phosphate removal. The results also showed that with an increase in the initial phosphate concentration, the dosage of adsorbed substance increased per gram of the adsorbent (adsorption capacity); this could be due to the initial phosphate concentration in the solutions that plays a key role as a driving force in overcoming the resistance caused by mass transfer between liquid and solid phases. Other research studies have reported similar results [63–65]. Also, Table 10 shows the phosphate adsorption capacity of various adsorbent. It should be noted that, in this study, adsorption capacity values were obtained using the minimum amount of surfactant concentration (equal to CMC of CTAB surfactant) and low percentage of nanoparticles which can increase the adsorption capacity by increasing the concentration of CTAB surfactant and increasing the percentage of nanoparticles in the modification of pumice aggregates.

Fig. 11 and Table 11 show the results of the investigation on Langmuir and Freundlich isotherms; the results show that given the obtained values of R_L and n , adsorp-

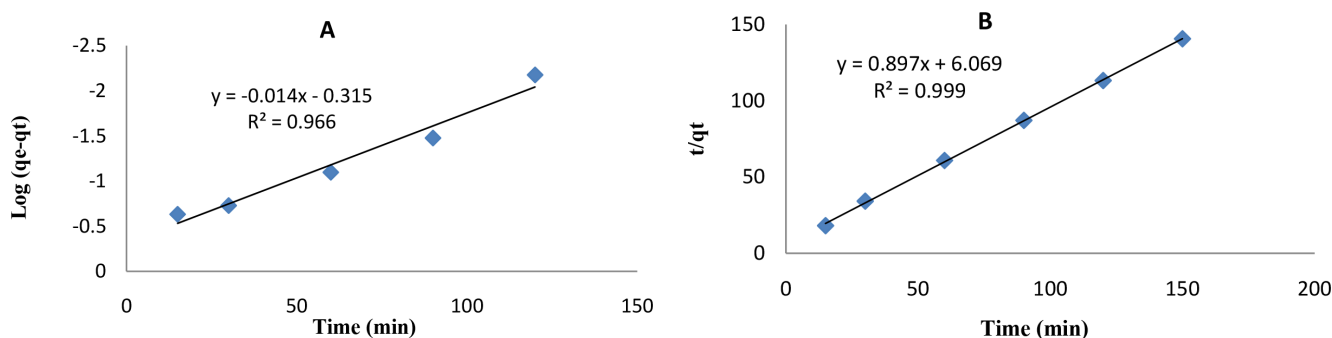


Fig. 9. The diagram of adsorption kinetic models (A: First order model, B: Second order model).

Table 8
Results of the first and second order adsorption kinetics

| Adsorbent | First order model | | | | Second order model | | | |
|---|-------------------|------------------------|----------------------------|----------------------------|--------------------|------------------------|----------------------------|----------------------|
| | R^2 | q_e (mg/g) Tested | q_e (mg/g) Calculated | K_1 (min ⁻¹) | R^2 | q_e (mg/g) Tested | q_e (mg/g) Calculated | K_2 (g/ mg·min) |
| Stabilized composite of zeolite nanoparticles modified on pumice aggregates | 0.96 | 1.066 | 0.483 | 0.033 | 0.99 | 1.066 | 1.113 | 0.132 |

Table 9
Results of different values of initial concentration on phosphate adsorption capacity under optimum conditions

| Absorbent | Initial concentration (mg/L) | Temperature (°C) | Absorbent dosage (g/L) | pH | Time (min) | Secondary concentration (mg/L) | q_e (mg/g) |
|-----------------|------------------------------|------------------|------------------------|----|------------|--------------------------------|-------------------|
| Modified pumice | 5 | 45 | 15 | 5 | 60 | 0.18 ± 0.036 | 0.321 ± 0.002 |
| | 10 | | | | | 0.90 ± 0.045 | 0.606 ± 0.003 |
| | 18 | | | | | 3.40 ± 0.070 | 0.973 ± 0.004 |
| | 28 | | | | | 12.4 ± 0.065 | 1.040 ± 0.004 |
| Natural pumice | 5 | 45 | 15 | 5 | 60 | 2.10 ± 0.026 | 0.193 ± 0.001 |
| | 10 | | | | | 4.90 ± 0.070 | 0.340 ± 0.004 |
| | 18 | | | | | 11.30 ± 0.065 | 0.446 ± 0.004 |
| | 28 | | | | | 21.10 ± 0.085 | 0.460 ± 0.005 |

*Each mean value (\pm standard deviation) was obtained from three repetitions.

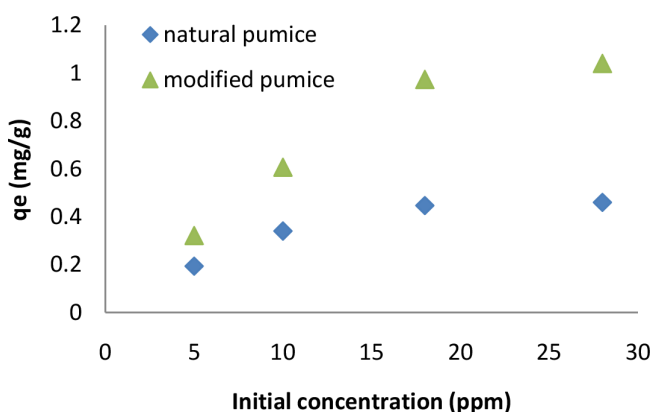


Fig. 10. Effects of different values of initial concentration on phosphate adsorption capacity under optimum conditions (pH = 5, temperature = 45°C, absorbent dosage = 15 g/L, and contact time = 60 min).

tion of both models have the optimum status; however, higher correlation coefficient of R^2 and closer values of adsorption capacity in Langmuir isotherm model with laboratory results show better agreement of data with Langmuir isotherm which describes the monotonous and homogenous distribution of active sites in the absorbent surface and it may be that phosphate adsorption is single-layer [71].

Table 10
Phosphate adsorption capacity of various adsorbent

| Adsorbent | q_e (mg/g) | Reference |
|----------------------------|--------------|------------|
| Kaolinite | 0.09 | 66 |
| Corn bio-char | 0.17 | 67 |
| Natural clinoptilolite | 0.65 | 68 |
| Montmorillonite | 0.74 | 66 |
| Magnetic orange peel | 1.24 | 69 |
| Coir-pith activated carbon | 1.61 | 70 |
| Natural pumice | 0.46 | This study |
| Modified pumice | 1.04 | This study |

3.7. Adsorption mechanism

In this study, the amount of phosphate adsorption capacity was very low by natural pumice aggregates. This value obtained low due to the presence of a structure of aluminosilicate in the natural pumice composition and its negative surface load, which causes a repulsive effect between the absorbent surface and the phosphate anions. However, the modification of zeolite nanoparticles by cationic surfactant CTAB and stabilization of nanoparticles on the surface of pumice aggregates increased the positive charge on the surface of pumice aggregates and improve the adsorption of phosphate anions by pumice aggregate. Generally, adsorption process can be interpreted by the three-step mechanism. In the first step, that is the general translocation step, the adsorbate is transferred to the adsorbent from the solution by mass transfer. In the second step, liquid molecular diffusion occurs in the pores. In the third step, adsorbate is adsorbed on the adsorbent surface. Many models for pollutants adsorption kinetic based on these mass transfer resistances are presented by researchers, which the first and second order adsorption kinetic models represent the third stage mechanism of the adsorption process [72] and the high matching of experiment data with second-order kinetic model shows that the adsorption phosphate mechanism was carried out through adsorption on the surface of adsorbent pores. In addition, the thermodynamic studies in experiment showed that the phosphate adsorption process is endothermic and the removal efficiency increases by increasing the temperature.

4. Conclusions

The results of the present study generally show that pumice modification by stabilizing zeolite nanoparticles increases the potential of phosphate adsorption. Results showed that a pH of 5, temperature of 45°C, and the absorbent dosage of 15 g/L are the optimum conditions for phosphate removal by stabilized composite of zeolite nanoparticles modified on pumice aggregate. Kinetic studies show that phosphate removal follows the second order model and the optimum contact time was measured at about 60 min where phosphate removal efficiency was 82.22%. It should be noted that the aforementioned con-

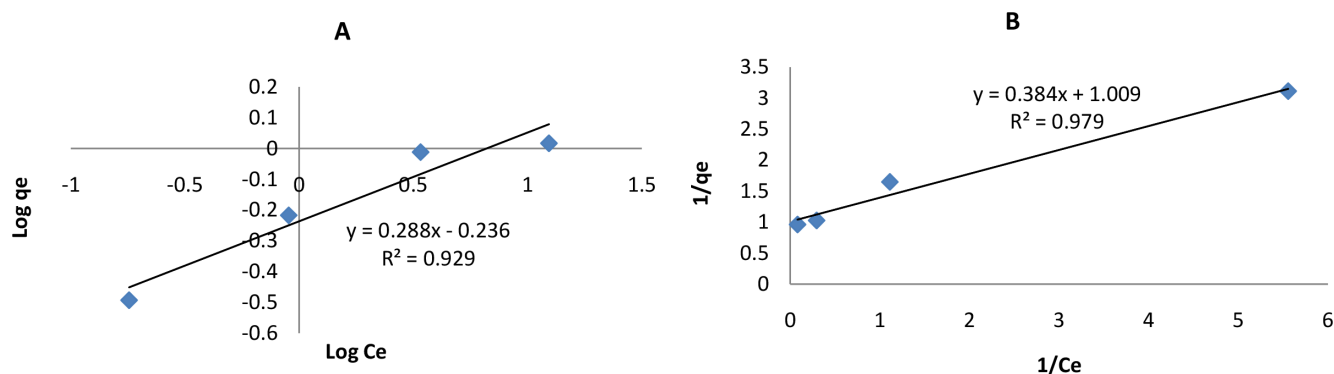


Fig. 11. The diagram of adsorption isotherm models (A: Freundlich isotherm, B: Langmuir isotherm).

Table 11
Results of Langmuir and Freundlich isotherm calculations

| Absorbent | Freundlich isotherm | | | Langmuir isotherm | | | |
|---|---------------------|----------|-----------------------------|-------------------|----------------------|-----------------------------|----------------------|
| | R ² | <i>n</i> | <i>K_f</i> (mg/g) | R ² | <i>R_L</i> | <i>q_m</i> (mg/g) | <i>K₁</i> |
| Stabilized composite of zeolite nanoparticles modified on pumice aggregates | 0.929 | 3.472 | 0.580 | 0.979 | 0.013 | 0.99 | 2.623 |

ditions not only increase the maximum adsorption efficiency, but also make it possible to reach higher values of removal efficiency under various conditions by thorough understanding and studying the performance and effects of parameters on each other. For example, at pH above 5, results show that removal level decreases, but, it is possible to reach a desirable level of removal efficiency by increasing the absorbent dosage. In conclusion, stabilized composite of zeolite nanoparticles modified on pumice aggregates is potentially capable of removing phosphate pollutant; given the high physical resistance, low price, cheap coverage, and its availability in nationwide mines, it could be a good option for developing the absorbents used by water and wastewater treatment refineries.

References

- [1] J. Ray, S. Jana, T. Tripathy, Synthesis of dipolar grafted hydroxyethyl cellulose and its application for the removal of phosphate ion from aqueous medium by adsorption, *Int. J. Biol. Macromol.*, 109 (2018) 492–506.
- [2] K. Karageorgiou, M. Paschalis, G. Anastassakis, Removal of phosphate species from solution by adsorption onto calcite used as natural adsorbent, *J. Hazard. Mater.*, 139 (2007) 447–452.
- [3] X. Yuan, W. Xia, J. An, J. Yin, X. Zhou, W. Yang, Kinetic and thermodynamic studies on the phosphate adsorption removal by dolomite mineral, *J. Chem-NY*, 2015 (2015) 1–8.
- [4] H. Yang, Q. Zhou, W. Luo, C. Yan, C. Zhou, The preparation of a cross-link cerium (III)-loaded alginate bead adsorbent for the removal of phosphate from wastewater, *Desal. Water Treat.*, 57(39) (2016) 18354–18365.
- [5] M. Parhamfar, A.B. Dalfard, M. Khaleghi, M. Hassanshahian, Isolation of phosphatase-producing phosphate solubilizing bacteria from Loriya spring: Investigation of phosphate solubilizing in the presence of different parameters, *Biol. J. Microorganism*, 3 (2014) 75–88.
- [6] W. Gu, X. Li, M. Xing, W. Fang, D. Wu, Removal of phosphate from water by amine-functionalized copper ferrite chelated with La (III), *Sci. Total Environ.*, 619 (2018) 42–48.
- [7] M. Lüring, E. Mackay, K. Reitzel, B.M. Spears, Editorial—a critical perspective on geo-engineering for eutrophication management in lakes, *Water Res.*, 97 (2016) 1–10.
- [8] J. Goscianska, M. Ptaszowska-Koniarz, M. Frankowski, M. Franus, R. Panek, W. Franus, Removal of phosphate from water by lanthanum-modified zeolites obtained from fly ash, *J. Colloid Interface Sci.*, 513 (2018) 72–81.
- [9] Z. Wang, D. Shen, F. Shen, T. Li, Phosphate adsorption on lanthanum loaded biochar, *Chemosphere*, 150 (2016) 1–7.
- [10] K. Kim, K. Kim, S. Asaoka, I.C. Lee, D.S. Kim, S. Hayakawa, Quantitative measurement on removal mechanisms of phosphate by class-F Fly Ash, *Int. j. Coal Prep. Util.*, 2018 (2018) 1–12.
- [11] X. Ren, C. Du, L. Zhang, Y. Zhuang, M. Xu, Removal of phosphate in aqueous solutions by the aluminum salt slag derived from the scrap aluminum melting process, *Desal. Water Treat.*, 57 (2016) 11291–11299.
- [12] K.W. Jung, T.U. Jeong, J.W. Choi, K.H. Ahn, S.H. Lee, Adsorption of phosphate from aqueous solution using electrochemically modified biochar calcium-alginate beads: Batch and fixed-bed column performance, *Bioresour. Technol.*, 244 (2017) 23–32.
- [13] H. Mahadevan, V.V. Dev, K.A. Krishnan, A. Abraham, O. Ershana, Optimization of retention of phosphate species onto a novel bentonite–alum adsorbent system, *Environ. Technol. Innovation*, 9 (2018) 1–15.
- [14] S. Hokkanen, E. Repo, L.J. Westholm, S. Lou, T. Sainio, M. Silanpää, Adsorption of Ni²⁺, Cd²⁺, PO₄³⁻ and NO₃⁻ from aqueous solutions by nanostructured micro fibrillated cellulose modified with carbonated hydroxyapatite, *Chem. Eng. J.*, 252 (2014) 64–74.
- [15] L. Fang, B. Wu, J.K. Chan, I.M. Lo, Lanthanum oxide nanorods for enhanced phosphate removal from sewage: A response surface methodology study, *Chemosphere*, 192 (2018) 209–216.
- [16] S. Mor, K. Chhoden, P. Negi, K. Ravindra, Utilization of nano-alumina and activated charcoal for phosphate removal from wastewater, *Environ. Nanotechnol. Monit. Manage.*, 7 (2017) 15–23.

- [17] Z. Guo, J. Li, Z. Guo, Q. Guo, B. Zhu, Phosphorus removal from aqueous solution in parent and aluminum-modified eggshells: thermodynamics and kinetics, adsorption mechanism, and diffusion process, *Environ. Sci. Pollut. Res.*, 24 (2017) 14525–14536.
- [18] J.K. Kim, S.B. Kim, S.H. Lee, J.W. Choi, Laboratory and pilot-scale field experiments for application of iron oxide nanoparticle-loaded chitosan composites to phosphate removal from natural water, *Environ. Technol.*, 39 (2018) 770–779.
- [19] T.H. Chen, J.Z. Wang, J. Wang, J.J. Xie, C.Z. Zhu, X.M. Zhan, Phosphorus removal from aqueous solutions containing low concentration of phosphate using pyrite calcinate sorbent, *Int. J. Environ. Sci. Technol.*, 12 (2015) 885–892.
- [20] D.K. Harijan, V. Chandra, Akaganeite nanorods decorated graphene oxide sheets for removal and recovery of aqueous phosphate, *J. Water Process Eng.*, 19 (2017) 120–125.
- [21] Y. Yang, J. Wang, X. Qian, Y. Shan, H. Zhang, Aminopropyl-functionalized mesoporous carbon (APTMS-CMK-3) as effective phosphate adsorbent, *Appl. Surf. Sci.*, 427 (2018) 206–214.
- [22] G. Asgari, B. Roshani, G. Ghanizadeh, The investigation of kinetic and isotherm of fluoride adsorption onto functionalize pumice stone, *J. Hazard. Mater.*, 217 (2012) 123–132.
- [23] Y. Pukcothanung, T. Siritanon, K. Rangriwatananon, The efficiency of zeolite Y and surfactant-modified zeolite Y for removal of 2, 4-dichlorophenoxyacetic acid and 1, 1'-dimethyl-4, 4'-bipyridinium ion, *Micropor. Mesopor. Mater.*, 258 (2018) 131–140.
- [24] M. Saltan, F.S. Findik, Stabilization of sub base layer materials with waste pumice in flexible pavement, *Build. Environ.*, 43 (2008) 415–421.
- [25] M. Nakhaeipour, F.A.H. Shojaee, F. Najarian, M. Safinezhad, H. Irvani, Determining the efficiency of zsm5-zeolite impregnated with nanoparticles of titanium dioxide in the photocatalytic removal of styrene vapors, *J. Occup. Hyg. Eng.*, 3 (2017) 61–67.
- [26] P.J. Reeve, H.J. Fallowfield, The toxicity of cationic surfactant HDTMA-Br, desorbed from surfactant modified zeolite, towards faecal indicator and environmental microorganisms, *J. Hazard. Mater.*, 339 (2017) 208–215.
- [27] M.R. Samarghandi, M. Tarlaniazar, R. Mehranpoor, M. Ahmadian, Survey the efficiency of iron-coated pumice in fluoride removal from aqueous solution, *J. Environ. Health Eng.*, 2 (2014) 128–140.
- [28] R.S. Bowman, Applications of surfactant-modified zeolites to environmental remediation, *Micropor. Mesopor. Mater.*, 61 (2003) 43–56.
- [29] G. Asgari, G. Ghanizadeh, A.S. Mohamadi, Adsorption of humic acid from aqueous solutions onto modified pumice with hexadecyl trimethyl ammonium bromide, *J. Babol Univ. Med. Sci.*, 14 (2011) 14–22.
- [30] F. Akbal, Sorption of phenol and 4-chlorophenol onto pumice treated with cationic surfactant, *J. Environ. Manage.*, 74 (2005) 239–244.
- [31] M.J. Khodayar, F. Namdar, S. Hojati, A. Landi, Z.N. Khorasgani, S. Alamolhoda, Removal of ametryn from aqueous solutions With zeolite nanoparticles optimized Using the box-Behnken design, *Jundishapur J. Nat. Pharm. Prod.*, 11 (2016) 1–9.
- [32] L.C. Wang, X.J. Ni, Y.H. Cao, G.Q. Cao, Adsorption behavior of bisphenol A on CTAB-modified graphite, *Appl. Surf. Sci.*, 428 (2018) 165–170.
- [33] A. Shil, S. Hussain, D. Bhattacharjee, Surfactant concentration dependent metachromasy of an anionic cyanine dye in adsorbed and deposited Langmuir films, *Chem. Phys. Lett.*, 676 (2017) 99–107.
- [34] U.O. Aigbe, R. Das, W.H. Ho, V. Srinivasu, A. Maity, A novel method for removal of Cr(VI) using polypyrrole magnetic nanocomposite in the presence of unsteady magnetic fields, *Sep. Purif. Technol.*, 194 (2018) 377–387.
- [35] I. Langmuir, The adsorption of gases on plane surfaces of glass, mica and platinum, *J. Am. Chem. Soc.*, 40 (1918) 1361–1403.
- [36] A. Karami, K. Karimyan, R. Davoodi, M. Karimaei, K. Sharafie, S. Rahimi, T. Khosravi, M. Miri, H. Sharafi, A. Azari, Application of response surface methodology for statistical analysis, modeling, and optimization of malachite green removal from aqueous solutions by manganese-modified pumice adsorbent, *Desal. Water Treat.*, 89 (2017) 150–161.
- [37] H. Yadaei, M.H. Beyki, F. Shemirani, S. Nouroozi, Ferrofluid mediated chitosan@ mesoporous carbon nanohybrid for green adsorption/preconcentration of toxic Cd (II): Modeling, kinetic and isotherm study, *React. Funct. Polym.*, 122 (2018) 85–97.
- [38] A.Q. Selim, E.A. Mohamed, M. Mobarak, A.M. Zayed, M.K. Seliem, S. Komarneni, Cr (VI) uptake by a composite of processed diatomite with MCM-41: isotherm, kinetic and thermodynamic studies, *Micropor. Mesopor. Mater.*, 260 (2018) 84–92.
- [39] H.M.F. Freundlich, over the adsorption in solution, *J. Phys. Chem.*, 57 (1906) 385–471.
- [40] M. Ligaray, C.M. Futralan, M.D. De Luna, M.W. Wan, Removal of chemical oxygen demand from thin-film transistor liquid-crystal display wastewater using chitosan-coated bentonite: Isotherm, kinetics and optimization studies, *J. Clean. Prod.*, 175 (2018) 145–154.
- [41] S. Mahdavi, D. Akhzari, The removal of phosphate from aqueous solutions using two nano-structures: copper oxide and carbon tubes, *Clean Technol. Environ. Pol.*, 18 (2016) 817–827.
- [42] A. Iriel, S.P. Bruneel, N. Schenone, A.F. Cirelli, The removal of fluoride from aqueous solution by a lateritic soil adsorption: Kinetic and equilibrium studies, *Ecotoxicol. Environ. Saf.*, 149 (2018) 166–172.
- [43] R.R. Kalantary, E. Dehghanifard, A. Mohseni-Bandpi, L. Rezaei, A. Esrafil, B. Kakavandi, A. Azari, Nitrate adsorption by synthetic activated carbon magnetic nanoparticles: kinetics, isotherms and thermodynamic studies, *Desal. Water Treat.*, 57 (2016) 16445–16455.
- [44] A. Azari, M. Gholami, Z. Torkshavand, A. Yari, E. Ahmadi, B. Kakavandi, Evaluation of basic violet 16 adsorption from aqueous solution by magnetic zero valent iron-activated carbon nanocomposite using response surface method: isotherm and kinetic studies, *J. Mazandaran Univ. Med. Sci.*, 24 (2015) 333–347.
- [45] L. Vafajoo, R. Cheraghi, R. Dabbagh, G. McKay, Removal of cobalt (II) ions from aqueous solutions utilizing the pre-treated 2-Hypnea Valentiae algae: Equilibrium, thermodynamic, and dynamic studies, *Chem. Eng. J.*, 331 (2018) 39–47.
- [46] M. Tuzen, A. Sari, T.A. Saleh, Response surface optimization, kinetic and thermodynamic studies for effective removal of rhodamine B by magnetic AC/CeO₂ nanocomposite, *J. Environ. Manage.*, 206 (2018) 170–177.
- [47] M.R. Samarghandi, M. Zarrabi, M.N. Sepehr, A. Amrane, G.H. Safari, S. Bashiri, Application of acidic treated pumice as an adsorbent for the removal of azo dye from aqueous solutions: kinetic, equilibrium and thermodynamic studies, *Iran. J. Environ. Health Sci. Eng.*, 9 (2012) 1–10.
- [48] M.H. Dehghani, M. Faraji, A. Mohammadi, H. Kamani, Optimization of fluoride adsorption onto natural and modified pumice using response surface methodology: Isotherm, kinetic and thermodynamic studies, *Korean J. Chem. Eng.*, 34 (2017) 454–462.
- [49] M. Zamparas, A. Gianni, P. Stathi, Y. Deligiannakis, I. Zacharias, Removal of phosphate from natural waters using innovative modified bentonites, *Appl. Clay Sci.*, 62 (2012) 101–106.
- [50] N. Kawasaka, F. Ogata, H. Tominaga, Selective adsorption behavior of phosphate onto aluminum hydroxide gel, *J. Hazard. Mater.*, 181 (2010) 574–579.
- [51] P. Castaldi, M. Silvetti, G. Garau, S. Deiana, Influence of the pH on the accumulation of phosphate by red mud (a bauxite ore processing waste), *J. Hazard. Mater.*, 182 (2010) 266–272.
- [52] M. Naushad, G. Sharma, A. Kumar, S. Sharma, A.A. Ghfar, A. Bhatnagar, F.J. Stadler, M.R. Khan, Efficient removal of toxic phosphate anions from aqueous environment using pectin based quaternary amino anion exchanger, *Int. J. Biol. Macromol.*, 106 (2018) 1–10.

- [53] J. Wang, Y. Liu, P. Hu, R. Huang, Adsorption of phosphate from aqueous solution by Zr (IV)-cross linked quaternized chitosan/bentonite composite, *Environ. Prog. Sustain. Ener.*, 37 (2018) 267–275.
- [54] A. Attour, M. Touati, M. Tlili, M.B. Amor, F. Lopicque, J.P. Leclerc, Influence of operating parameters on phosphate removal from water by electro coagulation using aluminum electrodes, *Sep. Purif. Technol.*, 123 (2014) 124–129.
- [55] M. Rashid, N.T. Price, M.Á.G. Pinilla, K.E. O’Shea, Effective removal of phosphate from aqueous solution using humic acid coated magnetite nanoparticles, *Water Res.*, 123 (2017) 353–360.
- [56] W. Huang, S. Wang, Z. Zhu, L. Li, X. Yao, V. Rudolph, F. Haghseresht, Phosphate removal from wastewater using red mud, *J. Hazard. Mater.*, 158 (2008) 35–42.
- [57] K.G. Scheckel, D.L. Sparks, Temperature effects on nickel sorption kinetics at the mineral–water interface, *Soil Sci. Soc. Am. J.*, 65 (2001) 719–728.
- [58] A.S. Özcan, A. Özcan, Adsorption of acid dyes from aqueous solutions onto acid-activated bentonite, *J. Colloid Interface Sci.*, 276 (2004) 39–46.
- [59] E. Unuabonah, K. Adebawale, B. Olu-Owolabi, L. Yang, L. Kong, Adsorption of Pb (II) and Cd (II) from aqueous solutions onto sodium tetraborate-modified kaolinite clay: equilibrium and thermodynamic studies, *Hydrometallurgy*, 93 (2008) 1–9.
- [60] L. Gan, Z. Lu, D. Cao, Z. Chen., Effects of cetyltrimethylammonium bromide on the morphology of green synthesized Fe_3O_4 nanoparticles used to remove phosphate, *Mater. Sci. Eng., C*, 82 (2018) 41–45.
- [61] S. Karaca, A. Gürses, M. Ejder, M. Açıkıldız, Adsorptive removal of phosphate from aqueous solutions using raw and calcinated dolomite, *J. Hazard. Mater.*, 128 (2006) 273–279.
- [62] Y. He, H. Lin, Y. Dong, L. Wang, Preferable adsorption of phosphate using lanthanum-incorporated porous zeolite: Characteristics and mechanism, *Appl. Surf. Sci.*, 426 (2017) 995–1004.
- [63] J. Zolgharnein, K. Dalvand, M. Rastgordani, P. Zolgharnein, Adsorptive removal of phosphate using nano cobalt hydroxide as a sorbent from aqueous solution; multivariate optimization and adsorption characterization, *J. Alloys Compd.*, 725 (2017) 1006–1017.
- [64] Y. Yao, B. Gao, M. Inyang, A.R. Zimmerman, X. Cao, P. Pullammanappallil, L. Yang, Removal of phosphate from aqueous solution by biochar derived from anaerobically digested sugar beet tailings, *J. Hazard. Mater.*, 190 (2011) 501–507.
- [65] S. Wang, L. Kong, J. Long, M. Su, Z. Diao, X. Chang, D. Chen, G. Song, K. Shih, Adsorption of phosphorus by calcium-flour biochar: Isotherm, kinetic and transformation studies, *Chemosphere*, 195 (2018) 666–672.
- [66] S. Tian, P. Jiang, P. Ning, Y. Su, Enhanced adsorption removal of phosphate from water by mixed lanthanum/aluminum pillared montmorillonite, *Chem. Eng. J.*, 151 (2009) 141–148.
- [67] D. Rajendra, Phosphate and nitrate removal from agricultural runoff by chitosan-graphite composite, *Res. Dev. Material Sci.*, 6 (2018) 1–11.
- [68] C. Tu, S. Wang, W. Qiu, R. Xie, B. Hu, G. Qu, P. Ning, Phosphorus removal from aqueous solution by adsorption onto La-modified clinoptilolite, *MATEC Web. Conf.*, 67 (2016) 1–14.
- [69] Q. Yang, X. Wang, W. Luo, J. Sun, Q. Xu, F. Chen, J. Zhao, S. Wang, F. Yao, D. Wang, X. Li, G. Zeng, Effectiveness and mechanisms of phosphate adsorption on iron-modified biochars derived from waste activated sludge, *Bioresour. Technol.*, 247 (2018) 537–544.
- [70] P. Kumar, S. Sudha, S. Chand, V.C. Srivastava, Phosphate removal from aqueous solution using coir-pith activated carbon, *Sep. Sci. Technol.*, 45 (2010) 1463–1470.
- [71] J. Wang, L. Wu, J. Li, D. Tang, G. Zhang, Simultaneous and efficient removal of fluoride and phosphate by Fe-La composite: Adsorption kinetics and mechanism, *J. Alloys Compd.*, 753 (2018) 422–432.
- [72] R.B. Garcia-Reyes, J.R. Rangel-Mendez, Adsorption kinetics of chromium (III) ions on agro-waste materials, *Bioresour. Technol.*, 101 (2010) 8099–8108.